Dinuclear Manganese(II) Complexes of Unsymmetric Phenol-based Dinucleating Ligands with Amino and Imino Chelating Arms: Synthesis, Structure and Catalase-like Activity†

Chikako Higuchi,[a] **Hiroshi Sakiyama,**[*,a] **Hisashi Ōkawa,**[*,a] **Ryuichi Isobe**[b] **and David E. Fenton**[c]
[a] *Department of Chemistry, Faculty of Science, Kyushu University, Hakozaki, Higashi-ku, Fukuoka 812, Japan*
[b] *Faculty of Pharmaceutical Sciences, Kyushu University, Maidashi, Higashi-ku, Fukuoka 812, Japan*
[c] *Department of Chemistry, The University of Sheffield, Sheffield S3 7HF, UK*

Unsymmetric phenol-based dinucleating ligands with amino and imino chelating arms, 4-bromo-2-{[(2-dimethylaminoethyl)methylamino]methyl}-6-[2-(dialkylamino)ethyliminomethyl]phenolate(1−) [alkyl = methyl (L^1) or ethyl (L^2)], formed dinuclear manganese(II) complexes $[Mn_2L(RCO_2)_2(NCS)]$ (L = L^1 or L^2, R = Me or Ph). The complex $[Mn_2L^2(MeCO_2)_2(NCS)]$ crystallizes in the monoclinic space group $P2_1/n$, a = 13.450(2), b = 18.743(3), c = 12.662(2) Å and β = 102.08(1)°. An X-ray diffraction analysis revealed that the dinuclear core structure is bridged by the phenolic oxygen of L^2 and by two acetate groups. The unsymmetric ligand provides different co-ordination geometries about the two manganese ions. The geometry of Mn at the imine site is distorted trigonal bipyramidal with the imine N and the two acetate O atoms in the basal plane and the phenolic O and the terminal N at the axial sites. The geometry of the Mn at the amine site is distorted octahedral involving also the nitrogen of the isothiocyanato group. Magnetic susceptibility measurements over the temperature range 4.2–300 K indicated weak antiferromagnetic interaction (J = −3 to −5 cm^{-1} based on $\hat{H} = -2JS_1 \cdot S_2$). Cyclic voltammetry for $[Mn_2L^1(MeCO_2)_2(NCS)]$ in CH_2Cl_2 revealed three quasi-reversible redox couples ($E_{\frac{1}{2}}$ = 0.63, 1.07 and 1.24 V *vs.* saturated calomel electrode) assignable to the stepwise oxidations $Mn^{II}Mn^{II} \longrightarrow Mn^{II}Mn^{III} \longrightarrow Mn^{III}Mn^{III} \longrightarrow Mn^{III}Mn^{IV}$. All the complexes show a catalase-like activity, disproportionating H_2O_2 into O_2 and H_2O. The presence of oxomanganese(IV) intermediates is suggested based on visible and mass spectrometric investigations.

Multinuclear manganese cores are known to play important roles in biological systems such as the oxygen-evolving complex of photosystem II,[1] manganese catalases[2] and manganese ribonucleotide reductase.[3] The catalase from *Thermus thermophilus*[4] is known to have two manganese(III) ions separated by 3.6(3) Å, and that from *Lactobacillus plantarum* also has two in each subunit.[5] For these a μ-oxo-bis(μ-carboxylato)-dimanganese(III) core structure is suggested based on visible spectral and extended X-ray absorption fine structure (EXAFS) studies,[6] however it is, as yet, unproven. The manganese content of manganese ribonucleotide reductase has not been determined but this metal enzyme is also suggested to contain a μ-oxo-bis(μ-carboxylato)-dimanganese(III) core.[6] Simple μ-oxo-bis(μ-carboxylato)-dimanganese-(III)[7] and -(III,IV)[8] complexes have been obtained as structural models but are unavailable for functional model studies because of their instability in solution, especially in the presence of hydrogen peroxide. At this stage it is of great value to use dinucleating ligands which provide a stable dinuclear core relevant to μ-oxo-bis(μ-carboxylato)-dimanganese(III).

Recently we have reported that μ-phenoxo-bis(μ-carboxylato)-dimanganese(II) complexes[9] derived from 2,6-bis[2-(dialkylamino)ethyliminomethyl]-4-methylphenol (alkyl = methyl or ethyl) are significantly stable in dimethylformamide (dmf) and show a catalase-like activity.[10] In the complexes of general formula $[Mn_2L(RCO_2)_2(NCS)]$ one manganese ion is five-co-ordinated (distorted trigonal bipyramidal) whereas the other is six-co-ordinated including the isothiocyanate nitrogen atom. In dmf they exist as $[Mn_2L(RCO_2)_2]^+$, of approximate C_s symmetry as judged from the crystal structure of $[Mn_2L(MeCO_2)_2(NCS)]$. Such C_s symmetry of $[Mn_2L(RCO_2)_2]^+$ is favourable for intramolecular interaction with hydrogen peroxide to provide a *cis*-$\{Mn^{III}(OH)\}_2$ and thence a *cis*-$\{Mn^{IV}(=O)\}_2$ core. Interconversion between these two cores results in the disproportionation of hydrogen peroxide.[10,11]

In this study on dinuclear manganese complexes we have adopted unsymmetric ligands 4-bromo-2-{[(2-dimethylaminoethyl)methylamino]methyl}-6-[2-(dialkylamino)ethyliminomethyl]phenol [alkyl = methyl (HL^1) or ethyl (HL^2)], which are analogues of 2,6-bis[2-(dialkylamino)ethyliminomethyl]-4-methylphenol [alkyl = methyl (HL^3) or ethyl], possessing one amino and one imino chelating arms in place of two imino chelating arms of the symmetric ligands. Dinuclear manganese(II) complexes $[Mn_2L(RCO_2)_2(NCS)]$ (L = L^1 or L^2, R = Me or Ph) have been obtained and the crystal structure of $[Mn_2L^2(MeCO_2)_2(NCS)]$ determined. The cryomagnetic (4.2–300 K) and electrochemical properties and the reactivity of the complexes toward H_2O_2 are described.

Experimental

Materials.—All the chemicals were of reagent grade and used as such.

---

† *Supplementary data available* (No. SUP 56993, 11 pp.): redox potentials, plots of magnetic data and oxygen evolution, EPR and mass spectra. See Instructions for Authors, *J. Chem. Soc., Dalton Trans.*, 1994, Issue 1, pp. xxiii–xxviii.

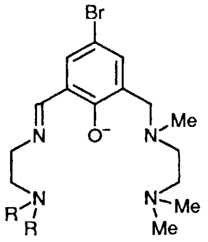

$(L^1)^-$ R = Me
$(L^2)^-$ R = Et

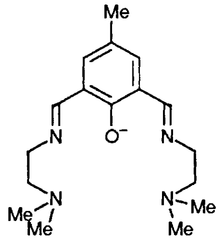

$(L^3)^-$

Measurements.—Elemental analyses of C, H and N were obtained at the Service Centre of Elemental Analysis, Kyushu University. Analyses of Mn were made on a Shimadzu AA-680 atomic absorption/flame emission spectrophotometer. Infrared spectra were recorded on KBr discs with a JASCO IR-810 spectrophotometer. Molar conductances were measured on a DKK AOL-10 conductivity meter at room temperature. Electronic spectra were recorded on a Shimadzu MPS-2000 spectrophotometer at room temperature, ^{1}H NMR spectra (400 MHz) on a JEOL JNM-GX 400 spectrometer in $CDCl_3$ using tetramethylsilane as the internal standard, electron impact (EI) mass spectra on a Hitachi M-60 mass spectrometer and fast atom bombardment (FAB) mass spectra on a JEOL JMS-SX102A/ 102A tandem mass spectrometer. Magnetic susceptibilities were measured on a HOXAN HSM-D SQUID susceptometer in the temperature range 4.2–80 K and a Faraday balance in the range 80–300 K. Calibrations were made with $[NH_4]_2Mn[SO_4]_2\cdot 6H_2O$ for the SQUID magnetometer and with $[Ni(en)_3][S_2O_3]$ (en = ethylenediamine) for the Faraday balance.[12] Effective magnetic moments were calculated by the equation $\mu_{eff} = 2.828(\chi_A T)^{\frac{1}{2}}$, where χ_A is the atomic magnetic susceptibility corrected for diamagnetism of the constituting atoms using Pascal's constants.[13] Cyclic voltammograms were recorded on an apparatus comprising a HA-501 potentiostat/galvanostat, a HB-104 function generator, and a HF-201 coulomb/amperehour meter of Hokuto Denko Ltd. Measurements were carried out in CH_2Cl_2 using a three-electrode cell equipped with a glassy carbon working electrode, platinum coil as the counter electrode and a saturated calomel electrode (SCE) as the reference. Tetra-*n*-butylammonium perchlorate was used as the supporting electrolyte. Controlled-potential electrolysis was performed on the same instrument using a platinum net as the working electrode.

Preparations.—*4-Bromo-2-[(2-dimethylaminoethyl)methylamino]methyl-6-formylphenol dihydrobromide*. This compound was prepared by a method similar to that of Crane *et al.*[14] 5-Bromosalicylaldehyde (10.0 g, 50 mmol), *N,N,N'*-trimethylethylenediamine (5.1 g, 50 mmol) and paraformaldehyde (2.0 g, 67 mmol) were refluxed in ethanol (150 cm^3) for 5 h to give an orange solution. The solution was cooled to room temperature and hydrobromic acid (48%, 15 cm^3) was added to give a pale yellow crystalline precipitate. Yield: 19.3 g (81%) (Found: C, 32.65; H, 4.65; N, 5.85. Calc. for $C_{13}H_{21}Br_3N_2O_2$: C, 32.75; H, 4.45; N, 5.85%).

The free form was obtained in 51% yield by neutralizing the dihydrobromide with $NaHCO_3$ (Found: C, 49.60; H, 6.10; N, 8.80. Calc. for $C_{13}H_{19}BrN_2O_2$: C, 49.55; H, 6.10; N, 8.90%). ^{1}H NMR ($CDCl_3$): δ 2.38 (d, 6 H), 2.60 (m, 4 H), 3.56 (s, 2 H), 7.33 (s, 1 H), 7.78 (d, 1 H) and 10.40 (s, 1 H). Positive EI mass spectrum: *m/z* 314 and 316.

$[Mn_2L^1(MeCO_2)_2(NCS)]$ **1**. A solution of the above dihydrobromide (0.239 g, 0.5 mmol), $LiOH\cdot H_2O$ (0.042 g, 1.0 mmol) and *N,N*-dimethylethylenediamine (0.044 g, 0.5 mmol) in methanol (10 cm^3) was refluxed for 20 min. To the resulting yellow solution was added manganese(II) acetate tetrahydrate (0.245 g, 1.0 mmol) and the mixture was refluxed for 30 min. The addition of NaSCN (0.081 g, 1.0 mmol) yielded yellow microcrystals. Yield: 0.167 g (50%) (Found: C, 39.30; H, 5.10; Mn, 16.20; N, 10.35. Calc. for $C_{22}H_{34}BrMn_2N_5O_5S$: C, 39.40; H, 5.10; Mn, 16.40; N, 10.45%). Selected IR data: 3000–2800, 2060, 1630, 1590, 1430, 1300, 1020 and 650 cm^{-1}. Molar conductance (Λ_M/S cm^2 mol^{-1}) in dmf: 57. VIS data [λ_{max}/nm (ε/dm^3 mol^{-1} cm^{-1})] in dmf: 355 (4700).

$[Mn_2L^2(MeCO_2)_2(NCS)]$ **2**. This complex was prepared as yellow microcrystals by a method similar to that for **1** using *N,N*-diethyl- instead of *N,N*-dimethyl-ethylenediamine. Yield: 0.236 g (68%) (Found: C, 41.10; H, 5.45; Mn, 15.75; N, 10.10. Calc. for $C_{24}H_{38}BrMn_2N_5O_5S$: C, 41.25; H, 5.50; Mn, 15.75; N, 10.05%). Selected IR data: 3000–2800, 2060, 1635, 1600, 1425, 1300, 1030 and 650 cm^{-1}. Molar conductance (Λ_M/S cm^2 mol^{-1}) in dmf: 67. VIS data [λ_{max}/nm (ε/dm^3 mol^{-1} cm^{-1})] in dmf: 360 (4900).

$[Mn_2L^1(PhCO_2)_2(NCS)]$ **3**. This complex was prepared as a yellow crystalline precipitate by a method similar to that for **1** using manganese(II) benzoate tetrahydrate instead of manganese(II) acetate tetrahydrate. Yield: 0.267 g (67%) (Found: C, 48.40; H, 4.90; Mn, 13.45; N, 8.80. Calc. for $C_{32}H_{38}BrMn_2N_5O_5S$: C, 48.40; H, 4.80; Mn, 13.85; N, 8.80%). Selected IR data: 3050–2800, 2065, 1635, 1610, 1570, 1460, 1410–1400, 1310, 1020, 720 and 680 cm^{-1}. Molar conductance (Λ_M/S cm^2 mol^{-1}) in dmf: 57. VIS data [λ_{max}/nm (ε/dm^3 mol^{-1} cm^{-1})] in dmf: 355 (4800).

$[Mn_2L^2(PhCO_2)_2(NCS)]$ **4**. This complex was prepared as a yellow crystalline precipitate by a method similar to that for **2**. Manganese(II) benzoate tetrahydrate was used instead of manganese(II) acetate tetrahydrate. Yield: 0.189 g (46%) (Found: C, 49.75; H, 5.20; Mn, 13.25; N, 8.45. Calc. for $C_{34}H_{42}BrMn_2N_5O_5S$: C, 49.65; H, 5.15; Mn, 13.35; N, 8.50%). Selected IR data: 3050–2800, 2050, 1640, 1605, 1565, 1450, 1410–1390, 1300, 710 and 670 cm^{-1}. Molar conductance (Λ_M/S cm^2 mol^{-1}) in dmf: 60. VIS data [λ_{max}/nm (ε/dm^3 mol^{-1} cm^{-1})] in dmf: 355 (5000).

X-Ray Structural Analysis of Complex **2**.—*Crystal data*. $C_{24}H_{38}BrMn_2N_5O_5S$, $M = 698.44$, monoclinic, space group $P2_1/n$, $a = 13.450(2)$, $b = 18.743(3)$, $c = 12.662(2)$ Å, $\beta = 102.08(1)°$, $U = 3121.4(9)$ Å^3, $D_m = 1.50$ g cm^{-3}, $Z = 4$, $D_c = 1.49$ g cm^{-3}, $F(000) = 1432$, μ(Mo-Kα) = 21.48 cm^{-1}.

Data collection and reduction. Single crystals of complex **2** were obtained by recrystallization from methanol–propan-2-ol (4:1). A crystal with approximate dimensions 0.4 × 0.4 × 0.4 mm sealed in a glass tube was used for the X-ray diffraction study. Intensities and lattice parameters were obtained on a Rigaku AFC-5 automated four-circle diffractometer, using graphite-monochromated Mo-Kα radiation ($\lambda = 0.710\,73$ Å) at 20 ± 1 °C. Lattice parameters and their estimated standard deviations were obtained from a least-squares fit to 25 reflections. For the intensity-data collection, the ω–2θ scan mode was used at a scan rate of 4° min^{-1}. The octant measured was $+h$, $+k$, $\pm l$. Three standard reflections were monitored every 100 and showed no systematic decrease in intensity. The intensity data were corrected for Lorentz and polarization factors and for absorption by Gaussian integration. 2667 Independent reflections with $F > 3\sigma(F)$ in the range $2.5 \leqslant 2\theta \leqslant 50°$ were assumed to be observed.

The structure was solved by direct methods. Refinement was carried out by the block-diagonal least-squares method, the function minimized being $\Sigma w(|F_o| - |F_c|)^2$ with $w = [\sigma(F_o)]^{-1}$. Atomic scattering factors were taken from ref. 15. Hydrogen atoms were fixed at the calculated positions and were not refined. The final values of R and R' were 0.0682 and 0.0650, respectively. All the calculations were carried out on a FACOM M-1800/20 computer in the Computer Centre of Kyushu University by the use of local versions[16] of the UNICS III[17] and ORTEP[18] programs.

The final positional parameters of the non-hydrogen atoms with their estimated standard deviations are listed in Table 1.

Additional material available from the Cambridge Crystallographic Data Centre comprises H-atom coordinates, thermal parameters, and remaining bond lengths and angles.

Results and Discussion

Structure of Complex **2**.—A perspective view of the complex molecule with the atom numbering scheme is depicted in Fig. 1. Selected bond distances and angles with their estimated standard deviations are listed in Table 2.

The complex molecule consists of the unsymmetric dinucleating ligand L^2, two manganese ions, two acetate groups, and one thiocyanate group. Atoms Mn(1) and Mn(2) are bridged by the phenolic oxygen of L^2 and two acetate groups, affording a μ-phenoxo-bis(μ-carboxylato)-dimanganese(II) core structure. The Mn(1) ··· Mn(2) distance is 3.376(2) Å, typical for this type of core structure.[9,19] The geometrical environments around Mn(1) and Mn(2) are different. That of Mn(1) is distorted trigonal bipyramidal with the imino nitrogen N(1) and the two acetate oxygens O(A1) and O(B1) in the basal plane and the phenolic oxygen O(1) and the amino nitrogen N(2) at the apices. The geometry of Mn(2) is distorted octahedral with the phenolic oxygen O(1) of L^2, amino nitrogens N(3) and N(4) of L^2, O(A2) and O(B2) of the bridging acetate groups, and N(5) of the isothiocyanato group.

A similar core structure with trigonal bipyramidal and octahedral manganese(II) ions has been observed for the related complex $[Mn_2L^3(MeCO_2)_2(NCS)]$ **5** with the symmetric dinucleating ligand $(L^3)^-$.[9]

The Mn–O distances [2.061(9)–2.214(7) Å] fall within the range commonly found for manganese(II) complexes.[20] The Mn(1)–N(1) [2.183(9) Å] and Mn(2)–N(3) [2.248(11) Å] distances are normal for manganese(II) complexes.[9,20] The distances Mn(1)–N(2) [2.318(8) Å] and Mn(2)–N(4) [2.354(9) Å] are slightly elongated probably because of the intramolecular steric repulsion between the substituents attached to the amino nitrogen and the bridging acetate groups. Similar elongation has been found in related dinuclear manganese(II) complexes.[9] The linearity of Mn–N–C–S is estimated by the bending angle θ between the two lines Mn–N and N–C–S obtained by the least-squares method. The value for **2** is 15.3° and that for **5** is 10.4°. This angle for other isothiocyanatomanganese(II) complexes[21–24] varies in a wide range (11.1–61.4°) and the values for **2** and **5** are thus rather small.

Physicochemical Properties.—All the dinuclear manganese(II) complexes **1**–**4** are air-stable in the solid state and in dmf solution. The IR spectrum of **1** shows the antisymmetric and symmetric $\nu(CO_2)$ vibrations of the acetate group at 1590 and 1430 cm^{-1}, respectively. Similarly, **2**–**4** show $\nu_{asym}(CO_2)$ and $\nu_{sym}(CO_2)$ vibrations of the carboxylate group at 1565–1600 and 1410–1430 cm^{-1}, respectively. The values of $\Delta\nu = \nu_{asym}(CO_2) - \nu_{sym}(CO_2)$ fall in a range 155–175 cm^{-1}. Values of $\Delta\nu$ smaller than 200 cm^{-1} are typical of bridging carboxylate groups.[25] This indicates that all the complexes have a μ-phenoxo-bis(μ-carboxylato)-dimanganese(II) core structure as demonstrated for **2** using X-ray crystallography. All the complexes show a strong peak at ≈2060 cm^{-1}, which is assigned to the ν(CN) of the isothiocyanato group. The ν(CS) and δ(NCS) modes of the isothiocyanato group could not be assigned unambiguously.

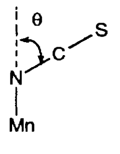

Magnetic susceptibility measurements were made on powder samples in the temperature range 4.2–300 K. The temperature dependences of the magnetic susceptibility (χ_A) and effective magnetic moment (μ_{eff}) per Mn for complex **1** are shown in Fig. 2. Corresponding curves for **2**–**4** are deposited as SUP 56993. The μ_{eff} values of the complexes at room temperature are in the

Table 1 Atomic coordinates (× 10^4) of non-hydrogen atoms in complex **2**

Atom	*x*	*y*	*z*
Mn(1)	7 132(1)	812(1)	−969(1)
Mn(2)	8 051(1)	1 174(1)	1 667(1)
Br	2 530(1)	2 068(1)	1 119(1)
O(1)	6 638(5)	1 207(4)	405(5)
N(1)	5 567(7)	427(5)	−1 394(7)
N(2)	6 949(7)	451(5)	−2 750(6)
N(3)	7 331(7)	2 085(5)	2 387(8)
N(4)	9 402(7)	1 606(6)	3 007(8)
C(1)	5 732(8)	1 404(6)	524(8)
C(2)	4 838(8)	1 091(6)	−91(8)
C(3)	3 892(8)	1 266(6)	128(9)
C(4)	3 820(9)	1 810(6)	858(9)
C(5)	4 688(9)	2 167(6)	1 377(9)
C(6)	5 629(9)	1 980(6)	1 226(8)
C(7)	4 806(9)	588(6)	−956(8)
C(8)	5 354(9)	−56(6)	−2 347(8)
C(9)	6 329(9)	−198(6)	−2 718(8)
C(10)	6 390(10)	1 024(6)	−3 451(9)
C(11)	6 069(11)	804(8)	−4 642(10)
C(12)	7 924(9)	237(7)	−3 052(9)
C(13)	8 604(10)	856(8)	−3 188(11)
C(14)	6 542(11)	2 426(8)	1 775(12)
C(15)	6 885(14)	1 834(12)	3 312(16)
C(16)	8 149(11)	2 559(7)	2 979(11)
C(17)	9 105(12)	2 213(11)	3 472(18)
C(18)	9 742(14)	961(14)	3 917(15)
C(19)	10 317(12)	1 704(11)	2 628(14)
O(A1)	8 025(6)	−51(5)	−373(6)
O(A2)	8 925(7)	348(5)	1 167(7)
C(A1)	9 330(11)	−780(8)	621(11)
C(A2)	8 708(9)	−99(7)	452(10)
O(B1)	7 895(7)	1 747(5)	−1 144(6)
O(B2)	8 580(7)	1 909(6)	564(7)
C(B1)	8 909(14)	2 756(8)	−657(12)
C(B2)	8 408(10)	2 076(8)	−387(9)
S	7 209(4)	−785(2)	3 859(4)
N(5)	7 456(9)	381(6)	2 609(9)
C(20)	7 375(10)	−103(7)	3 124(10)

Table 2 Selected bond distances (Å) and angles (°) of complex **2**

Mn(1)–O(1)	2.121(8)	Mn(1)–N(1)	2.183(9)
Mn(1)–N(2)	2.318(8)	Mn(1)–O(A1)	2.061(9)
Mn(1)–O(B1)	2.066(9)	Mn(2)–O(1)	2.214(7)
Mn(2)–N(3)	2.248(11)	Mn(2)–N(4)	2.354(9)
Mn(2)–O(A2)	2.119(11)	Mn(2)–O(B2)	2.184(10)
Mn(2)–N(5)	2.126(12)	Mn(1) ··· Mn(2)	3.376(2)
O(1)–Mn(1)–N(1)	82.3(3)	O(1)–Mn(1)–N(2)	155.8(3)
O(1)–Mn(1)–O(A1)	103.4(3)	O(1)–Mn(1)–O(B1)	92.3(3)
N(1)–Mn(1)–N(2)	76.3(3)	N(1)–Mn(1)–O(A1)	106.8(3)
N(1)–Mn(1)–O(B1)	136.7(4)	N(2)–Mn(1)–O(A1)	93.6(3)
N(2)–Mn(1)–O(B1)	95.6(3)	O(A1)–Mn(1)–O(B1)	116.2(4)
O(1)–Mn(2)–N(3)	83.9(3)	O(1)–Mn(2)–N(4)	158.0(4)
O(1)–Mn(2)–O(A2)	104.6(3)	O(1)–Mn(2)–O(B2)	82.8(3)
O(1)–Mn(2)–N(5)	93.2(4)	N(3)–Mn(2)–N(4)	77.3(4)
N(3)–Mn(2)–O(A2)	171.5(3)	N(3)–Mn(2)–O(B2)	90.4(4)
N(3)–Mn(2)–N(5)	93.3(4)	N(4)–Mn(2)–O(A2)	94.2(4)
N(4)–Mn(2)–O(B2)	86.5(4)	N(4)–Mn(2)–N(5)	99.1(4)
O(A2)–Mn(2)–O(B2)	89.7(4)	O(A2)–Mn(2)–N(5)	87.4(4)
O(B2)–Mn(2)–N(5)	173.9(4)		

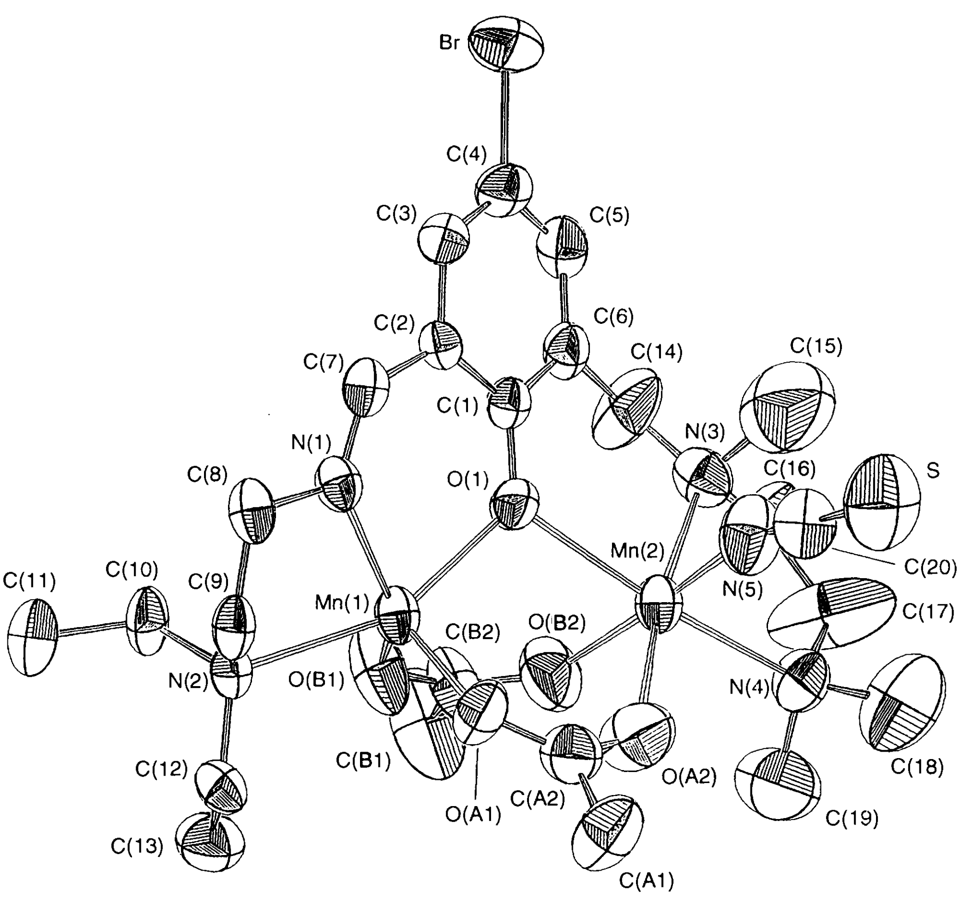

Fig. 1 ORTEP view of complex **2** with the atom numbering scheme

range 5.47–5.56 μ_B (Table 3) and decrease with lowering of temperature. The results suggest that the manganese(II) ion has high spin in all the complexes and there is an antiferromagnetic interaction between pairs of manganese(II) ions. The magnetic susceptibility equation based on the Heisenberg model $\hat{H} = -2JS_1 \cdot S_2$ ($S_1 = S_2 = \frac{5}{2}$) is given in (1) where $x = \exp(-J/kT)$

$$\chi_A = \frac{Ng^2\beta^2}{kT} \cdot \frac{x^{28} + 5x^{24} + 14x^{18} + 30x^{10} + 55}{x^{30} + 3x^{28} + 5x^{24} + 7x^{18} + 9x^{10} + 11} + N_\alpha \quad (1)$$

and other symbols have their usual meanings. The cryomagnetic property of **1** is well simulated by this equation, using the magnetic parameters $g = 2.00$, $J = -4.9$ cm^{-1}, and $N_\alpha = 0$ cm^3 mol^{-1}. The discrepancy factor defined as $R(\mu) = [\Sigma(\mu_{obs} - \mu_{calc})^2/\Sigma(\mu_{obs})^2]^{\frac{1}{2}}$ was 3.5×10^{-3}. Similarly, good magnetic simulations have been attained for **2**–**4**. The best-fitting parameters obtained for those complexes are summarized in Table 3. The exchange integrals J fall in the range -3 to -5 cm^{-1} and are comparable to the values for other μ-phenoxo-bis(μ-carboxylato)-dimanganese(II) complexes ($J = -2$ to -5 cm^{-1}) derived from $(L^3)^-$ and a homologue[9] and 4-methyl-2,6-bis[2-(2-pyridyl)ethyliminomethyl]phenolate(1−).[19]

All the complexes show no appreciable absorption in the region above 450 nm in dmf solution, in accord with the high-spin electronic configuration of Mn^{II}. An intense absorption band observed around 360 nm is assigned to the azomethine π–π* transition.[26]

From the molar conductance data all the complexes are found to act as 1:1 electrolytes in dmf.[27] This suggests dissociation of the NCS$^-$ group. In the FAB mass spectrum of 3

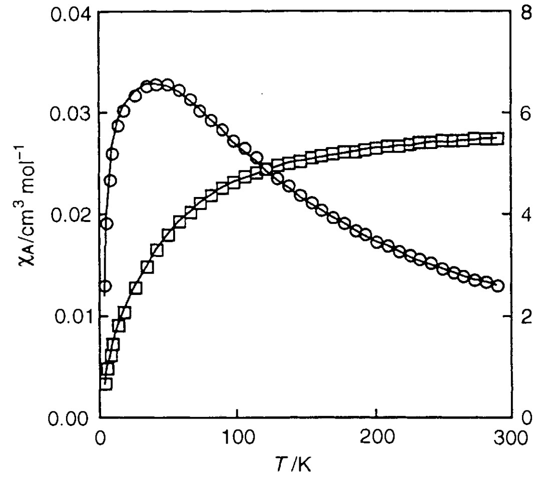

Fig. 2 Temperature dependences of χ_A (○) and μ_{eff} (□) of complex **1**. Solid curves are based on equation (1), using $J = -4.9$ cm^{-1}, $g = 2.00$ and $N_\alpha = 0$

Table 3 Magnetic data for complexes **1**–**4***

Complex	μ_{eff}/μ_B at room temperature	J/ cm^{-1}	g	$10^{-3}R(\mu)$
1 [Mn$_2$L^1(MeCO$_2$)$_2$(NCS)]	5.49	−4.9	2.00	3.5
2 [Mn$_2$L^2(MeCO$_2$)$_2$(NCS)]	5.53	−3.2	1.98	6.5
3 [Mn$_2$L^1(PhCO$_2$)$_2$(NCS)]	5.56	−4.1	2.00	4.0
4 [Mn$_2$L^2(PhCO$_2$)$_2$(NCS)]	5.47	−4.8	2.00	6.4

* N_α fixed at 0 cm^3 mol^{-1}.

in dmf the most predominant ions appeared at m/z 735 and 737 corresponding to $[Mn_2L^1(PhCO_2)_2]^+$. The appearance of two peaks is due to the presence of ^{79}Br and ^{81}Br in L^1.

Electrochemistry.—Cyclic voltammograms of complex **1** in CH_2Cl_2 with tetra-*n*-butylammonium perchlorate as the supporting electrolyte are shown in Fig. 3. At a scan rate of 400 mV s^{-1} there are three quasi-reversible redox couples (i–iii) at $E_{\frac{1}{2}}$ = 0.63, 1.07 and 1.24 V *vs.* SCE, respectively [see Fig. 3(*a*)]. The first is found to be a one-electron-transfer process from coulometry at 0.60 V *vs.* SCE. The EPR spectrum (SUP 56993) at 77 K for the one-electron oxidized solution shows a multiline signal superposed on a broad signal around $g \approx 2$, suggesting the presence of a $Mn^{II}Mn^{III}$ species. Thus, the first couple may be assigned to the process $Mn^{II}Mn^{II} \longrightarrow Mn^{II}Mn^{III}$. Couples ii and iii are tentatively assigned to $Mn^{II}Mn^{III} \longrightarrow Mn^{III}Mn^{III}$ and $Mn^{III}Mn^{III} \longrightarrow Mn^{III}Mn^{IV}$, respectively. At a scan rate of 50 mV s^{-1} couple iii practically disappears while i and ii remain [Fig. 3(*b*)]. The scan rate dependence of the cyclic voltammogram suggests that the $Mn^{III}Mn^{III}$ species formed on the electrode undergoes a chemical reaction such as disproportionation or intramolecular electron transfer.

In the case of complex **3** two quasi-reversible redox couples are observed at $E_{\frac{1}{2}}$ = 0.60 and 1.06 V *vs.* SCE, corresponding to the first two redox couples (i and ii) of **1**. Cyclic voltammograms of the related complex **5** show three ill defined redox couples around 0.45, 0.60 and 0.85 V *vs.* SCE. Similarly, the cyclic voltammogram of $[Mn_2L^3(PhCO_2)_2(NCS)]$ **6** shows an ill defined quasi-reversible couple at $E_{\frac{1}{2}}$ = 0.54 V *vs.* SCE and two anodic peaks at 0.85 and 1.02 V. Complexes **5** and **6** with the symmetric Schiff-base ligand $(L^3)^-$ are oxidized to $Mn^{II}Mn^{III}$ complexes more easily than are **1** and **3** with the unsymmetric ligand $(L^1)^-$. This may be attributed to the electronic effect of the *para*-substituent on the phenol ring of the dinucleating ligand. That is, $(L^1)^-$ with the electron-withdrawing bromo group stabilizes the low-valent Mn^{2+} state relative to $(L^3)^-$ with the electron-donating methyl group. The separation between the potentials of the first two couples is 0.44 and 0.46 V *vs.* SCE for **1** and **3**, respectively. These separations are large compared with those of **5** and **6** (0.14 and < 0.3 V *vs.* SCE, respectively). It is evident that the mixed-valence $Mn^{II}Mn^{III}$ state is stabilized with the unsymmetric ligand $(L^1)^-$ relative to the symmetric ligand $(L^3)^-$.

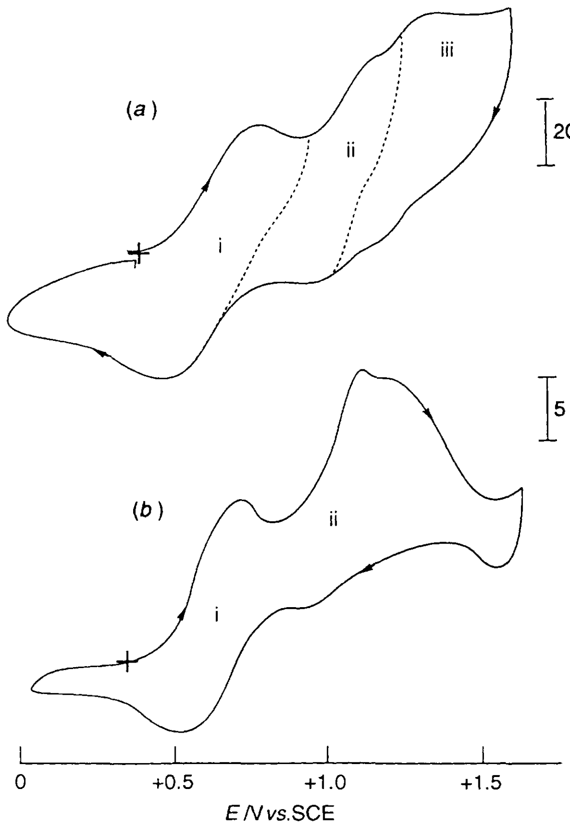

Fig. 3 Cyclic voltammograms of complex **1** in CH_2Cl_2 containing 0.1 mol dm^{-3} NBu_4ClO_4 on a glassy-carbon electrode at scan rates (*a*) 400 and (*b*) 50 mV s^{-1}. The dotted curves in (*a*) indicate the cyclic voltammograms measured for the first two couples

Reaction with Hydrogen Peroxide.—The catalase-like activity of complexes **1**–**4** was examined in dmf solutions by volumetric measurements of evolved dioxygen. An example of the time course of this is given in Fig. 4. All the complexes decompose H_2O_2 catalytically [equation (2)]. The time course of dioxygen

$$2H_2O_2 \longrightarrow O_2 + 2H_2O \qquad (2)$$

evolution by complexes **1**–**4** is sigmoidal with a slow initial process A and the much faster process B appearing after a lag. The initial rate v_A and the maximum rate v_{max} were obtained based on the least-squares method and the rate of reaction B, v_B, is determined by the relation $v_B = v_{max} - v_A$. The induction period of reaction B, τ, was determined graphically (see Fig. 4). The values of v_A, v_B and τ for each complex are summarized in Table 4.

In this paper only the initial rate v_A will be discussed because v_B and τ are dependent upon factors such as the populations of the ionic species associated with reactions A and B, the stability of each active species, the concentration of H_2O_2, *etc.* From Table 4 it appears that the initial rate v_A for complexes **1**–**4** is sensitive to steric features of the complex molecule. The value for the L^1 complex is larger than that of the L^2 complex when comparing the complexes with the same bridging carboxylate group, *i.e.* **1** > **2** and **3** > **4**. This is in accord with the increasing

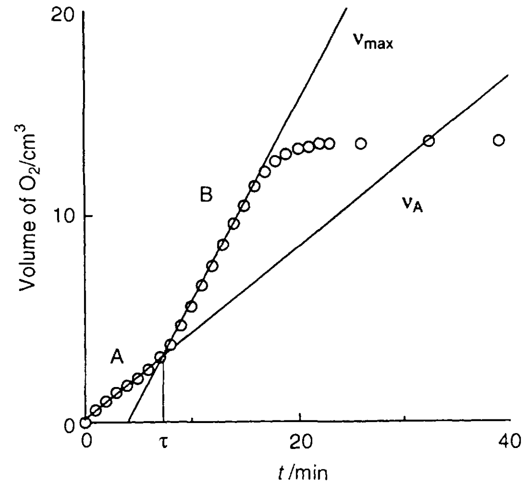

Fig. 4 Time course of dioxygen evolution in H_2O_2 disproportionation by complex **2**. Conditions: **2** (5 μmol) in dmf (2 cm^3), H_2O_2 (10.0%, 0.5 cm^3; 1.45 mmol), at 0 °C. $v_B = v_{max} - v_A$

Table 4 Rates of dioxygen evolution v_A and v_B and the induction period τ for complexes **1**–**4**

Complex	v_A*	v_B*	τ/min
1	36	21	6
2	16	25	7
3	23	40	9
4	10	37	9

* μmol min^{-1}.

size of the nitrogen substituent (methyl for L^1 and ethyl for L^2). Further, the acetate complex shows a larger ν_A value than that of the benzoato complex when comparing complexes of the same dinucleating ligand, *i.e.* **1** > **3** and **2** > **4**. This is also in accord with the increasing bulkiness of the bridging group. These results are regarded as evidence that process A proceeds by an inner-sphere mechanism and the approach of H_2O_2 to the metal centre is subject to steric hindrance from the substituent at nitrogen and the residue of the carboxylate group.

The time course of dioxygen evolution for complexes **1**–**4** is very similar to that of **6**.[10] In the catalase-like reaction of **6** the intermediates $[Mn^{II}Mn^{IV}({=}O)L^3(PhCO_2)_2]^+$ and $[\{Mn^{IV}({=}O)\}_2L^3(PhCO_2)_2]^+$ have been detected in processes A and B, respectively, based on visible and FAB mass spectrometry.[10]

The visible spectral changes during the H_2O_2 disproportionation reaction with complex **3** are shown in Fig. 5. Immediately after the addition of H_2O_2 the solution became yellow but changed to pink after an induction period. The pink solution showed an intense absorption band (ε = *ca.* 3800 $dm^3 mol^{-1} cm^{-1}$) around 530 nm upon which fine structures, separated by *ca.* 730 cm^{-1}, were imposed (see Fig. 5). The fine structure may be assigned to the ν(Mn=O) vibration coupled to a ligand-to-metal charge-transfer (l.m.c.t.) (from O^{2-} to Mn^{IV}) band through vibronic interaction.[10] The other complexes also showed a similar spectral change and the numerical data are summarized in Table 5. The intensity of the l.m.c.t. band, calculated on the initial concentration of the dinuclear manganese(II) complex, varies probably due to the different concentrations of the pink species.

The pink solution formed on adding H_2O_2 to the dmf solution of complex **3** was subjected to FAB mass spectrometry, three pairs of significant ions (*m*/*z* 719, 721; 735, 737; and 751, 753) being detected in the mass range 700–800 (see Fig. 6). In the absence of H_2O_2, **3** shows only one pair of ions (*m*/*z* 735, 737) which is assigned to $[Mn_2L^1(PhCO_2)_2]^+$ (M^+) as mentioned above. The new species (*m*/*z* 719, 721) can be assigned to $[M - CH_3 - H]^+$, which may be formed by oxidative elimination of the methyl group on the articular nitrogen. Therefore, the species with *m*/*z* 735, 737 can be assigned to $[M + O - CH_3 - H]^+$ and/or intact $[M]^+$, and that with *m*/*z* 751, 753 to $[M + 2O - CH_3 - H]^+$ and/or $[M + O]^+$. Thus, it is suggested that three species $[M]^+$, $[M + O]^+$ and $[M + 2O]^+$ exist in the pink solution. The presence of the ν(Mn=O) vibration on the l.m.c.t. band adds support to the formation of oxomanganese(IV) species.

One noticeable difference in catalase-like activity between complexes **1**–**4** and **6** is that the total amount of evolved O_2 was 60–70% of the theoretical amount for **1**–**4** whereas it was 100% for **6**.[10] It should be emphasized that in the reaction with **1**–**4** no H_2O_2 remained when the evolution of O_2 had ceased. In this disproportionation a side reaction consuming H_2O_2 through a one-electron transfer process is believed to occur. Also that in the catalase-like disproportionation of H_2O_2 into O_2 and H_2O two-electron oxidation and reduction processes are essential [equations (3) and (4)]. At this stage we only point out that **1**–**4**

$$H_2O_2 - 2e^- \longrightarrow O_2 + 2H^+ \qquad (3)$$

$$H_2O_2 + 2H^+ + 2e^- \longrightarrow 2H_2O \qquad (4)$$

differ from **6** in electrochemical properties, stabilizing the $Mn^{II}Mn^{III}$ mixed-valence state which can be associated with the one-electron transfer.

Acknowledgements

We thank Miss Mie Tomono for ^1H NMR and EI mass spectral measurements, and Mr. Masaaki Ohba for the help in magnetic measurements. This work was supported by a Grant-in-Aid for Scientific Research on Priority Area (No. 03241105) and by Fellowships of the Japan Society for the Promotion of Science for Japanese Junior Scientists (No. 1985).

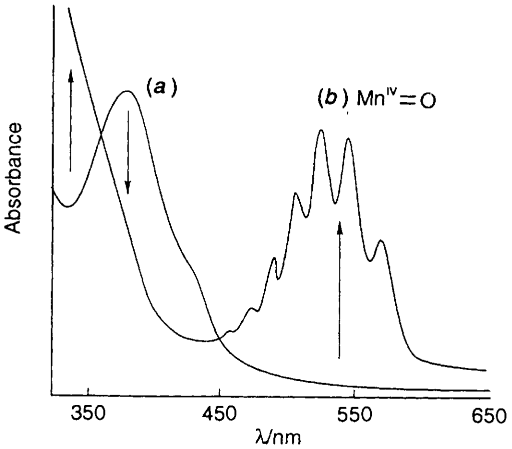

Fig. 5 Visible spectral changes on adding H_2O_2 (10.0%, 0.5 cm^3) to a dmf solution of complex **3** (10^{-4} mol dm^{-3}, 2 cm^3): (*a*) just after the addition of H_2O_2, (*b*) after 20 min

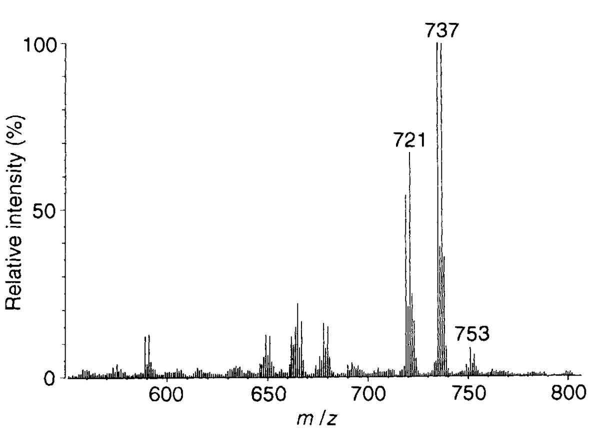

Fig. 6 Positive-ion FAB mass spectrum of an aqueous dmf solution of complex **3** and H_2O_2 with a *m*-nitrobenzyl alcohol matrix. Conditions: **3** (*ca.* 0.07 μmol) in dmf (*ca.* 0.05 cm^3), H_2O_2 (10%, *ca.* 0.05 cm^3; *ca.* 40 μmol), after *ca.* 10 min

Table 5 Wavenumber (ν_{av}) of the vibration and the molar absorption coefficients ε of the l.m.c.t. band for complexes **1**–**4**

Complex	ν_{av}/cm^{-1}	$\varepsilon_{max}/$ $dm^3 mol^{-1} cm^{-1}$
1	727	1500
2	736	390
3	733	3800
4	730	1100

References

1 G. C. Dismukes, *Photochem. Photobiol.*, 1986, **43**, 99.
2 R. M. Fronko, J. E. Penner-Hahn and C. J. Bender, *J. Am. Chem. Soc.*, 1988, **110**, 7554; G. S. Allgood and J. J. Perry, *J. Bacteriol.*, 1986, **168**, 563.
3 A. Willing, H. Follmann and G. Auling, *Eur. J. Biochem.*, 1988, **170**, 603.
4 V. V. Barynin, A. A. Vagin, V. R. Melik-Adamyan, A. I. Grebenko, S. V. Khangulov, A. N. Popov, M. E. Andrianova and B. K. Vainshtein, *Sov. Phys. Dokl.*, 1986, **31**, 457.
5 Y. Kono and I. Fridovich, *J. Biol. Chem.*, 1983, **258**, 13646; W. F. Beyer, jun., and I. Fridovich, *Biochemistry*, 1985, **24**, 6460.
6 K. Wieghardt, *Angew. Chem., Int. Ed. Engl.*, 1153, **28**, 1989; V. L. Pecoraro, *Manganese Redox Enzymes*, VCH, Weinheim, 1992.
7 K. Wieghardt, U. Bossek, D. Ventur and J. Weiss, *J. Chem. Soc.*,

Chem. Commun., 1985, 347; K. Wieghardt, U. Bossek, B. Nuber, J. Weiss, J. Bonvoisin, M. Corbella, S. E. Vitols and J.-J. Girerd, *J. Am. Chem. Soc.*, 1988, **110**, 7398; S. Menage, J. J. Girerd and A. Gleizes, *J. Chem. Soc., Chem. Commun.*, 1988, 431; Y. Nishida, N. Oshio and T. Tokii, *Z. Naturforsch., Teil B*, 1988, **43**, 637.

8 K. Wieghardt, U. Bossek, J. Bonvoisin, P. Beauvillain, J. J. Girerd, B. Nuber, J. Weiss and J. Heinze, *Angew. Chem.*, 1986, **98**, 1026; *Angew. Chem., Int. Ed. Engl.*, 1986, **25**, 1030.

9 H. Sakiyama, H. Tamaki, M. Kodera, N. Matsumoto and H. Ōkawa, *J. Chem. Soc., Dalton Trans.*, 1993, 591.

10 H. Sakiyama, H. Ōkawa and R. Isobe, *J. Chem. Soc., Chem. Commun.*, 1993, 882.

11 H. Sakiyama, H. Ōkawa and M. Suzuki, *J. Chem. Soc., Dalton Trans.*, 1993, 3823.

12 L. F. Lindoy, V. Katovic and D. H. Busch, *J. Chem. Educ.*, 1972, **49**, 117.

13 E. A. Boudreaux and L. N. Mulay, *Theory and Applications of Molecular Paramagnetism*, Wiley, 1976, p. 491.

14 J. D. Crane, D. E. Fenton, J. M. Latour and A. J. Smith, *J. Chem. Soc., Dalton Trans.*, 1991, 2979.

15 *International Tables for X-Ray Crystallography*, Kynoch Press, Birmingham, 1974, vol. 4.

16 S. Kawano, *Rep. Comput. Cent., Kyushu Univ.*, 1983, **16**, 113.

17 T. Sakurai and K. Kobayashi, *Rep. Inst. Phys. Chem. Res.*, 1979, **55**, 69.

18 C. K. Johnson, Report No. ORNL3794, Oak Ridge National Laboratory, Oak Ridge, TN, 1965.

19 M. Mikuriya, T. Fujii, S. Kamisawa, Y. Kawasaki, T. Tokii and H. Oshio, *Chem. Lett.*, 1990, 1181.

20 B. Mabad, P. Cassoux, J.-P. Tuchagues and D. N. Hendrickson, *Inorg. Chem.*, 1986, **25**, 1420.

21 D. W. Engelfriet, G. C. Verschoor and W. J. Vermin, *Acta Crystallogr., Sect. B*, 1979, **35**, 2927.

22 M. V. Veidis, B. Dockum, F. F. Charron, jun., and W. M. Reiff, *Inorg. Chim. Acta*, 1981, **53**, L197.

23 M. G. B. Drew, A. H. bin Othman, S. G. McFall, P. D. A. McIlroy and S. M. Nelson, *J. Chem. Soc., Dalton Trans.*, 1977, 438.

24 M. G. B. Drew, A. H. bin Othman, S. G. McFall, P. D. A. McIlroy and S. M. Nelson, *J. Chem. Soc., Dalton Trans.*, 1977, 1173.

25 G. B. Deacon and R. J. Phillips, *Coord. Chem. Rev.*, 1980, **32**, 227.

26 B. Bosnich, *J. Am. Chem. Soc.*, 1968, **90**, 627.

27 W. J. Geary, *Coord. Chem. Rev.*, 1971, **7**, 81.

Received 31*st August* 1993; *Paper* 3/05224I